Monatsh Chem
DOI 10.1007/s00706-016-1835-2

ORIGINAL PAPER

Synthesis, characterization, crystal structure, and DNA interaction of tin complexes containing pyridyl ligands

Badri Z. Momeni[1] · **Vahid Noroozi**[1]

Received: 19 February 2016 / Accepted: 9 August 2016

Abstract The reactions of 4′-aryl-2,2′:6′,2″-terpyridines (aryl = phenyl, *p*-tolyl, *p*-anisyl, *p*-chlorophenyl, 4-pyridyl) and 3-phenyl-1,5-bis(2-pyridyl)-1,5-pentanedione with dimethyltin(IV) dichloride and tin(II) dichloride have been investigated. The resulting products have been fully characterized by elemental analysis and multinuclear (^{1}H, ^{13}C, ^{119}Sn) NMR spectroscopy and X-ray crystal structure determination in the case of [$SnCl_2$(pytpy)] (pytpy = 4′-(4-pyridyl)-2,2′:6′,2″-terpyridine). The crystal structure of [$SnCl_2$(pytpy)] reveals that tin(II) is pentacoordinated in a highly distorted square pyramidal geometry. Moreover, the binding interaction of complex [$SnCl_2$(pytpy)] with calf thymus-DNA (ct-DNA) has been investigated using UV–Vis spectroscopy. Data reveals that the groove binding is a mode of the interaction with a moderate binding constant of 7.2 (±0.2) × 10^3 M^{-1}.

Graphical abstract

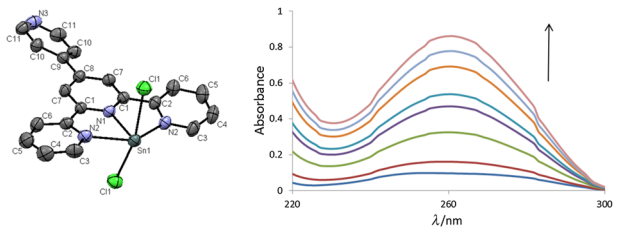

Electronic supplementary material The online version of this article (doi:10.1007/s00706-016-1835-2) contains supplementary material, which is available to authorized users.

✉ Badri Z. Momeni
momeni@kntu.ac.ir

[1] Faculty of Chemistry, K. N. Toosi University of Technology, P.O. Box 16315-1618, Tehran 15418, Iran

Keywords Tin · Terpyridyl · NMR · Crystal structure · DNA

Introduction

The diversity of applications related to terpyridines and their metal complexes calls for a high structural variability of the basic 2,2′:6′,2″-terpyridine subunit. In fact, terpyridine units have been incorporated into supramolecular dendrimers [1–4] and polymers [5–7]. In particular, nowadays, terpyridine designs featuring π-conjugated substituents, commonly attached in 4′ position, are of increasing interest. In the field of metallo-supramolecular chemistry, 4′-functionalized terpyridines have favorite properties to be employed in structure, and a multitude of terpyridine-functionalized polymers has been derived from this structural motif [8–13]. By far, the most conjugated terpyridine-containing systems used today are based on the so-called Kröhnke-motif, which features a functionalized phenyl moiety at the 4′-position of the terpyridine unit [14].

Tin complexes are an attended family of compounds, with dominant applications in chemical vapor deposition (CVD), PVC stabilizers, chemical sensors, nonlinear optics, supramoleculer structures, as well as organic synthesis and catalysis [15]. Also, they are potentially suitable for medicinal and biocidal purposes, due to their biological activity [16, 17]. In addition, the organotin complexes containing *N*-donor ligands show anticancer activity [18, 19]. Widespread antitumor studies of tin complexes have attracted interests to design complexes specially using *N*-donor ligands, to follow the structures of cisplatin family model [15]. However, activity of tin(II) complexes of *N*-donor ligands, such as terpyridines (as multiple *N*-donors) because of the capability to bind

Published online: 31 August 2016

through the nitrogens of DNA base pairs, or other interacting modes may have noticeable results for this purpose.

In one of previous research reports on organotin terpyridine complexes, Lewis has studied the effect of dimethyltin(IV) as a transient template in condensation of ligand [20]. In another report, the cytotoxicity of fluorescent organotin complexes of terpyridine derivatives have been studied [21]. Also, we have studied the preparation of dimethyltin(IV) complexes based on the pyridyl ligands using different spectroscopic methods and X-ray crystallography to demonstrate the geometry of the resulting complexes which indicated that the functional group on terpyridine ligand affects the coordination geometry of tin(IV) in solution and the counterion [22].

In this paper, we have studied the synthesis of dimethyltin(IV) dichloride and tin(II) dichloride complexes containing a series of pyridyl ligands (4′-aryl-2,2′:6′,2″-terpyridines (aryl = phenyl (Phtpy) **L1**, *p*-tolyl (toltpy) **L2**, *p*-anisyl (atpy) **L3**, *p*-chlorophenyl (CPtpy) **L4**, 4-pyridyl (pytpy) **L5**), and 3-phenyl-1,5-bis(2-pyridyl)-1,5-pentanedione (**L6**); Scheme 1) to demonstrate the solution behavior and coordination geometry of prepared complexes using spectroscopy and crystallography, besides the binding interaction study of complex **5** with DNA.

Results and discussion

All adducts of organotin(IV) and tin(II) dichlorides have been prepared by the reaction of proper amounts of multidentate polypyridyl ligands **L1**–**L6** with dimethyltin(IV) and tin(II) compounds. In the case of dimethyltin(IV), formation of terpyridyl complexes has been shown in Scheme 2. Then, the products were fully characterized by elemental analysis, IR spectroscopy, ^{1}H, ^{13}C, and ^{119}Sn NMR spectroscopy, and single crystal X-ray diffraction analysis in the case of [$SnCl_2$(pytpy)]. Also, the interaction of ct-DNA with complex **5** has been studied using UV–Vis spectroscopy.

Solution studies

The study of prepared complexes **1**–**6** in solution, their characterization and structural behavior in this state was done by multinuclear NMR spectroscopy, including ^{1}H, ^{13}C, and ^{119}Sn. Assignments of the ^{1}H and ^{13}C NMR spectra were mainly based on the previous published data for free ligands [23, 24].

The ^{1}H NMR spectra of all complexes can be assigned based on two distinguished regions of aromatic and aliphatic (methyl) functional groups. While the comparison of the spectra of ligands and related complexes confirms the complex formation, assignments were done based on the spectral patterns of free ligands and dimethyltin(IV) dichloride in above two regions.

Information about the structure of methyltin(IV) compounds in solution can be also drawn from the coupling constants for the methyl carbons bonded to tin and the tin-hydrogen coupling. Details of the mechanism are available in the literature [25, 26]. The $^{119/117}Sn$ satellites were identified based on the previous observations [27]. It is revealed that the magnitude of tin–hydrogen coupling constant ^{2}J (^{119}Sn–^{1}H), is also related to Me–Sn–Me angle [28]:

$$\theta = (0.0161)\left[{}^{2}J\left({}^{119}Sn-{}^{1}H\right)\right]^{2} - (1.32)\left[{}^{2}J\left({}^{119}Sn-{}^{1}H\right)\right] + 133.4 \quad (1)$$

It has also been found that the magnitude of ^{1}J (^{119}Sn-^{13}C) is linearly related to the Me–Sn–Me bond

Scheme 1

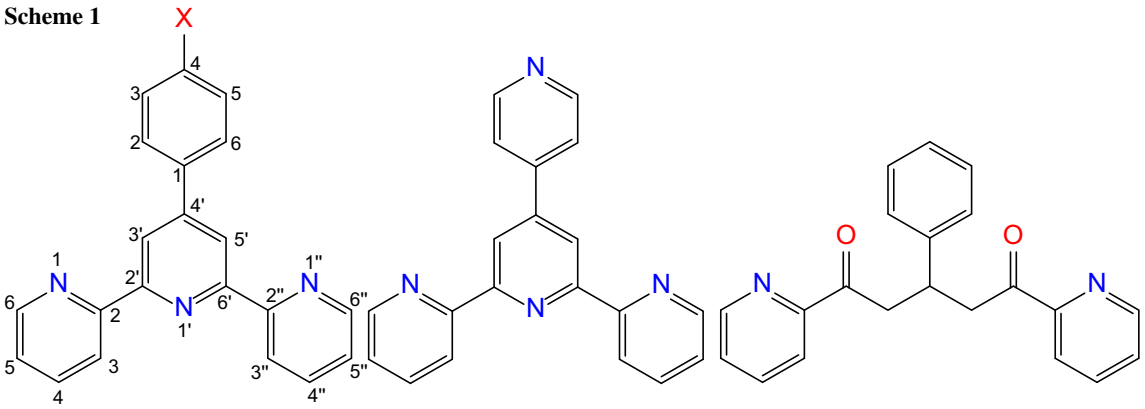

Scheme 2

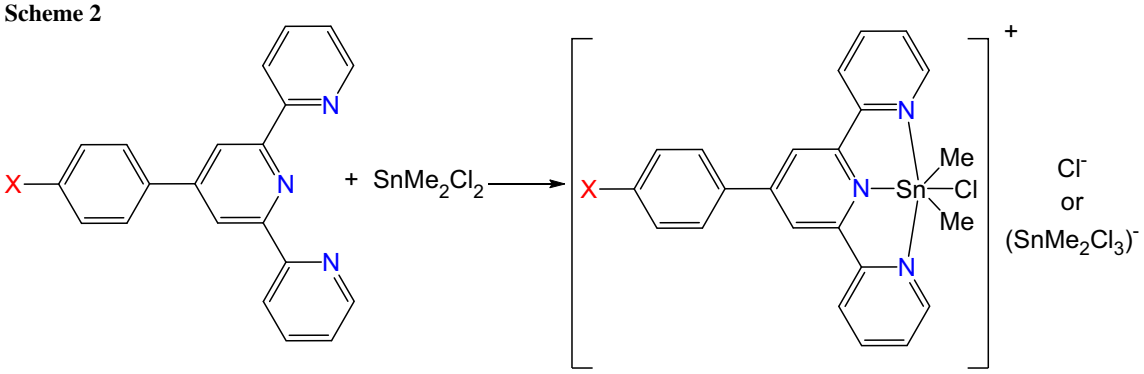

Table 1 ^{1}H chemical shifts and coupling constants, $^{2}J(^{119/117}\text{Sn–H})$, for prepared organotin(IV) complexes

Compound	Solvent	Chemical shift/δ	^{2}J ($^{119/117}$Sn–H)/Hz
Me_2SnCl_2	$CDCl_3$	1.19	68.6/65.7
1	$CDCl_3$	1.23	90.6
2	$CDCl_3$	1.20	93.2
3	$CDCl_3$	1.21	92.5
4	$CDCl_3$	1.23	89.5/86.2
	Acetone	1.16	94.6/90.7
6	Acetone	1.21	85.4

angle, θ, in tetra-, penta-, and hexa-coordinated di-, tri-, and tetramethyltin(IV) (Eq. 2) [29]:

$$^{1}J\left(^{119}Sn-^{13}C\right) = 11.4\theta - 875 \quad (2)$$

The ^{1}H NMR spectrum of each one of the prepared complexes shows signal at $\delta \sim 1.20$ ppm for methyl groups connected to tin(IV), with coupling constants over two bonds $^{2}J(^{119/117}\text{Sn}–^{1}\text{H})$, in the range of 85.4 Hz $<^{2}J$ ($^{119/117}$Sn–H) <94.6 Hz (Table 1) different from the coupling constants of primary compound Me_2SnCl_2, which are ^{2}J (^{119}Sn–H) = 68.6 and $^{2}J(^{117}\text{Sn}–\text{H}) = 65.7$ Hz in $CDCl_3$ [30]. Application of Eq. (1) for complex **3** results in $\theta \sim 149.1°$ (based on $^{2}J(^{119}\text{Sn}–^{1}\text{H}) = 92.5$ Hz) and Eq. (2) results in $\theta \sim 145.8°$ (based on $^{1}J(^{119}\text{Sn}–^{13}\text{C}) = 787$ Hz), which both are resulting in solution state and the difference is less than 5°.

The ^{1}H NMR spectra of the complexes **2** and **3** in $CDCl_3$ display a singlet at $\delta = 2.43$ ppm and a singlet at 3.71 ppm, respectively; according to methyl and methoxy on *para* positions of phenyl groups [31].

Structural difference of complexes **1–4** is only in substitutions on *para* position of the phenyl groups, so it is expectable to have similar electronic environments, and therefore similarity in the positions of spectral signals of the equivalent pyridyl rings. This subject is slightly obvious in ^{1}H NMR spectra and more clearly in ^{13}C NMR spectra, and sometimes deviation from this issue occurs when there is also sensitivity to the type of the solvents. For instance, for complex **4**, $H_{3',5'}$ singlet peak shifts to downfield when acetone is used instead of chloroform as NMR solvent. Since there are data for approximate calculation of chemical shifts of benzene derivatives [31], it is possible to predict chemical shifts for the positions on phenyl groups with low deviations, both in ^{1}H and in ^{13}C NMR. Moreover, in the case of ^{13}C NMR of complexes **1** and **2**, DEPTQ-135 experiment was used for assignment of carbons with confidence.

The ^{119}Sn NMR spectra of complexes **1–3** in $CDCl_3$ show signals at $\delta = -121$, -116, and -121 ppm, respectively, which are in the range of five-coordinated tin(IV) centers. Also, complexes **2** and **3** show other signals, respectively, at -64 and -69 ppm. The ^{119}Sn NMR spectrum of **4** in acetone-d_6 shows a weak signal at -150 ppm and an unexpected signal at -632 ppm that is remarkably more negative than six-coordinated tin(IV) chemical shift and its value is comparable with heptacoordinated tin(IV), despite difference with previous reports [32]. Moreover, ^{119}Sn NMR spectroscopy of complex **5** in DMSO indicates a shifted peak to upfield at -630 ppm which is associated with coordinative capability of DMSO to interact with tin center [15].

Also, the study of complex **6** by ^{119}Sn NMR shows a signal at +10 ppm that is identified as a four-coordinated tin(IV) center in acetone-d_6 solution. It is noticeable that it differs with the primary four-coordinated $SnMe_2Cl_2$ compound that shows a signal at $\delta(^{119}\text{Sn}) = +137$ ppm in dichloromethane solution [33]. Elemental analysis data suggests that complex **6** might be as [$SnMe_2Cl$(**L6**)]Cl·**L6**, and ^{13}C NMR data confirms it and shows the presence of free ligand as cocrystal in complex **6**. ^{13}C NMR data of complex **6** has two series of peaks, one series for the half of bonded to organotin(IV) and other series related to head not in complex that are also common with free ligand. We have reported similar kind of structure previously [22]. The ^{1}H NMR spectra of complex **6** shows a singlet at 1.21 ppm

and its satellites with $^{2}J(^{119/117}\text{Sn–H}) = 85.4$ Hz are observable. This value, besides other near ^{2}J values in this range for complexes **1**–**4**, proposes hexacoordinated environment for tin centers in solution. However, this is just a qualitative indication [34]. Also, it is noteworthy that ^{1}H NMR spectra have been determined immediately after resolving in solvent, but in the case of ^{119}Sn and ^{13}C NMR, the spectra have been determined overnight that increases the chance of dissociation and might reduce the coordination number.

^{119}Sn NMR spectroscopy results mention that the studied chemical species have different complicated structural behavior in solution state, especially the fact that all complexes dissociate to ionic species in solution. This was also confirmed qualitatively by preliminary conductivity measurements of the complexes **1**–**3** in distilled water, acetone, and $CHCl_3$. The conductivity test shows an order of conductance for these complexes: **3** ~ **1** > **2**, while solutions in water rationally had the most conductance (i.e., **3**: 820 μS, **1**: 810 μS, and **2**: 490 μS for 2 mM solutions in water).

DNA binding studies

The binding of ct-DNA with metal complex was studied using electronic absorption spectroscopy. Absorption spectra were recorded for varying concentrations of complex **5** and ct-DNA to obtain different ratios of ct-DNA: complex mixtures. The results have been shown in Fig. 1. The intrinsic binding constant, K_B, was measured with an approach by considering the observed absorbance values as well as initial concentrations of complex **5** and ct-DNA solutions in equilibrium equations (S1–S5). The method performed by employing the spreadsheet Excel program to analyze data and calculate K_B based on some different initial guess of binding constant and extinction coefficient of ct-DNA-complex **5** as two variables using Solver option to minimize the sum of standard deviations (S7) of experimental and calculated absorbance (S6) in each spectrum at 260 nm. Also, the results show good curve fitting for calculated and experimental absorbance data, in Fig. S1 (more details are available in Supplementary Material). This method is effective since the whole components in solution (i.e., ct-DNA, complex **5** and their combined compound) have absorbance in the studied UV–Vis area.

The resulting K_B value is $7.2(\pm0.2) \times 10^3$ M^{-1}. This value is comparable with the reported values for compounds $[Zn(Phtpy)Cl_2]$ (1.60×10^3 M^{-1}), $[Cd(Phtpy)_2](NO_3)_2$ (7.42×10^3 M^{-1}) [35], $[Pt(tpy)(SC_4H_9)]^+$ (8.4×10^3 M^{-1}); $[Pt(tpy)(OH)]^+$ (7×10^4 M^{-1}); $[Pt(tpy)Cys]^+$ (1.0×10^5 M^{-1}) [36]. Also, its value is between tin(II) complexes of $[Sn(oda)(bpy)(H_2O)_2]$ (5.35×10^3 M^{-1}) and $[Sn(oda)(phen)(H_2O)_2]$ (2.52×10^4 M^{-1}) (phen (1,10-phenanthroline), bpy (2,2′- bipyridine), and oda (oxydiacetate)) [37].

Addition of increasing amounts of ct-DNA to solutions of complex **5** resulted in the obvious hyperchromism tendency of the absorption bands at 260 nm, which has the characteristic of ct-DNA. However, since the tin(II) complex spectrum has a maximum absorbance band at 244 nm, there is no subject to conclude that the band shifted to 260 nm is a reason for bathochromic effect of intercalating mode of action. Moreover, the hyperchromic effect with a significant red shift may suggest a binding propensity to ct-DNA, possibly by electrostatic interaction, and stabilization of the complex DNA adducts [38]. Also, hypochromism in time dependent spectra of 1:1 molar ratio for ct-DNA: complex **5** (Fig. 2) was observed. Generally, this indication arises from a contraction in the helix axis of ct-DNA [39]. So, it is more likely to consider the interaction of ct-DNA and the complex **5** as groove binding (non-

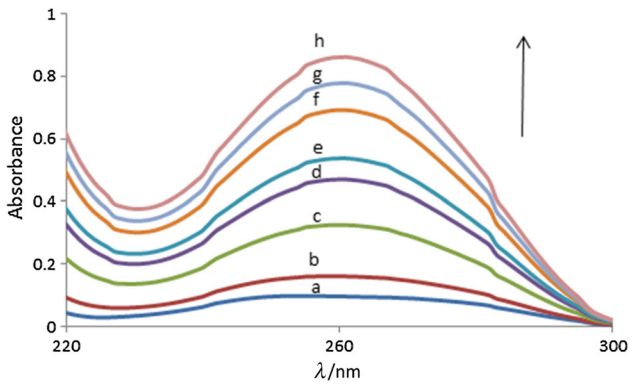

Fig. 1 Absorption spectra of ct-DNA and tin (II) complex solutions; *arrow* shows the increasing amounts of ct-DNA: metal complex ratios [$r_i = 4.96n$; $n = 1$–8 (*a*–*h*]

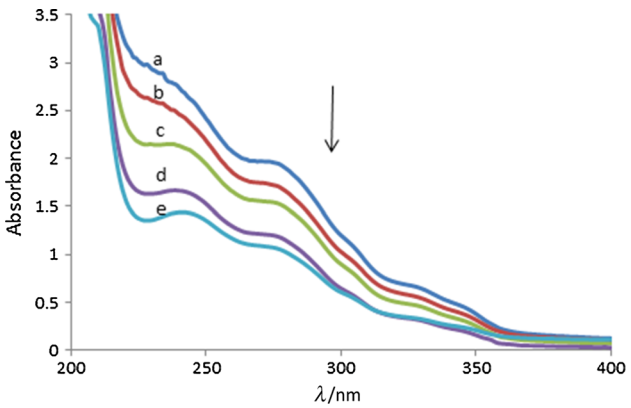

Fig. 2 Absorption spectra of the 1:1 molar ratio solution of ct-DNA and tin (II) complex ($c = 2.90 \times 10^{-5}$ M); *arrow* shows obvious decrease in the absorbance intensity after passing specific time periods (for 2 (*a*), 7 (*b*), 17 (*c*), 32 (*d*) and 55 (*e*) min after mixing)

intercalative), despite the capability of the ligand part of the complex (pytpy) to interact with base pairs.

From the value of the binding constant (K_B), Gibbs free energy (ΔG) of the complex DNA compound can be calculated using Eq. (3):

$$\Delta G = -\mathrm{RT} \ln K_B \quad (3)$$

Binding constant represents the bound compound stability while the free energy indicates the spontaneity or non-spontaneity of complex DNA binding. The free energy value, -22.02 kJ mol^{-1}, shows the spontaneity of the interaction [40].

Description and discussion of the crystal structure of 5

The molecular structure of [$SnCl_2$(pytpy)] (**5**) is shown in Fig. 3. The coordination geometry around Sn(II) can be described as significantly distorted square pyramidal, since its geometry parameter $\tau = 0.39$ ($\tau = (\beta - \alpha)/60°$, where β and α are the largest two angles in the coordination center; $\tau = 0$ for a perfect square pyramidal and 1 for a perfect trigonal bipyramidal [41, 42]). Nitrogen atom of the middle pyridyl ring occupies axial position, while other coordinated atoms, 2N and 2Cl, build up the equatorial plane. In complex **5** similar to other tin(II) complexes, the coordination sphere includes space for the stereochemically active lone electron pair [15]. Different examples of 2-, 3-, 4-, 6-, 7-, and 8-coordinate tin(II) complexes are known [43], and complex **5** is one of the rare examples of reported five-coordinate tin(II) complexes with a terpyridyl ligand [44]. As it is obvious in crystal data, a position seems not coordinated around Sn(II), even with the presence of an expanded ligand (**L5**), which has one extra *N*-donor site in comparison with other terpyridines, and potential of connection to a metal center.

In distorted square pyramidal geometry around Sn(II), two chlorine atoms have occupied *trans* positions and the Cl(1)-Sn-Cl(1^{i}) angle is 159.85° which significantly deviates from linearity. Other *trans* positions occupied by nitrogen atoms show N(2)–Sn(1)–N(2^{i}) angle of 136.45° which is significantly nonlinear, and steric effect of rigid *N*-donation sites are responsible for it. Dihedral angles of two connected rings in coordinated side of the ligand, C(7)–C(1)–C(2)–C(6) and N(1)–C(1)–C(2)–N(2) are 7.8° and 7.3°, respectively. It shows three pyridyl rings with slightly nonparallel configuration. In previous report [44], the side rings have 4.2° angles with central ring, when the ligand is just 2,2′:6′,2″-terpyridine. However, the fourth, non-coordinated pyridyl ring is significantly out of the plane and C(10)–(C9)–C(8)–C(7) dihedral angle is 23.6°. All bond lengths are quite near to similar ones in reported structure [44]. For instance, Sn(1)–N(1), Sn(1)–N(2), and Sn(1)–Cl(1) bonds, with 2.336, 2.382, and 2.688 Å lengths, respectively, have inconsiderable differences with bond distances reported previously.

The pyridyl–terpyridine ligands in three dimensional crystal structure of the complex **5** lie in antiparallel layers, as is obvious in Fig. 4, which is viewed down through the axis b.

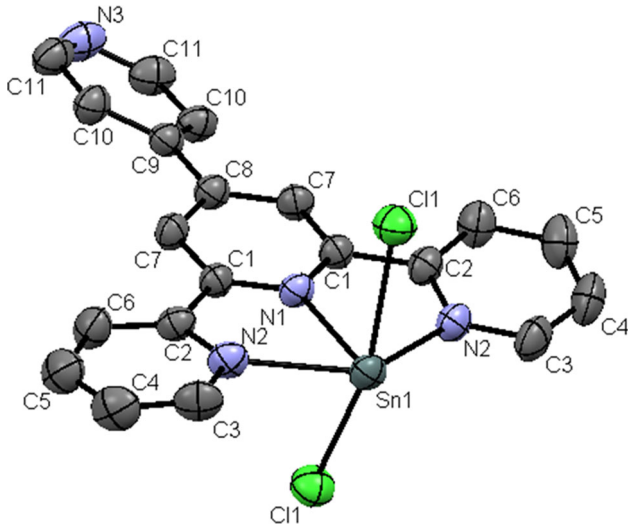

Fig. 3 ORTEP diagram for [$SnCl_2$(pytpy)]. Selected bond distances (Å) Sn(1)–N(1) 2.336(3), Sn(1)–N(2) 2.382(3), Sn(1)–Cl(1) 2.6879(9). Selected bond angles (°) N(1)–Sn(1)–N(2) 68.23(6), N(2)–Sn(1)–N(2^{i}) 136.45(12), N(1)–Sn(1)–Cl(1) 79.93(2), N(2)–Sn(1)–Cl(1) 83.67(7), N(2^{i})–Sn(1)–Cl(1) 88.88(7), N(1)–Sn(1)–Cl(1) 79.93(2), Cl(1)–Sn(1)–Cl(1^{i}) 159.85(4), C(1)–N(1)–C(1^{i}) 119.3(3), C(1)–N(1)–Sn(1) 120.37(17), C(3)–N(2)–Sn(1) 120.5(2), C(2)–N(2)–Sn(1) 119.5(2)

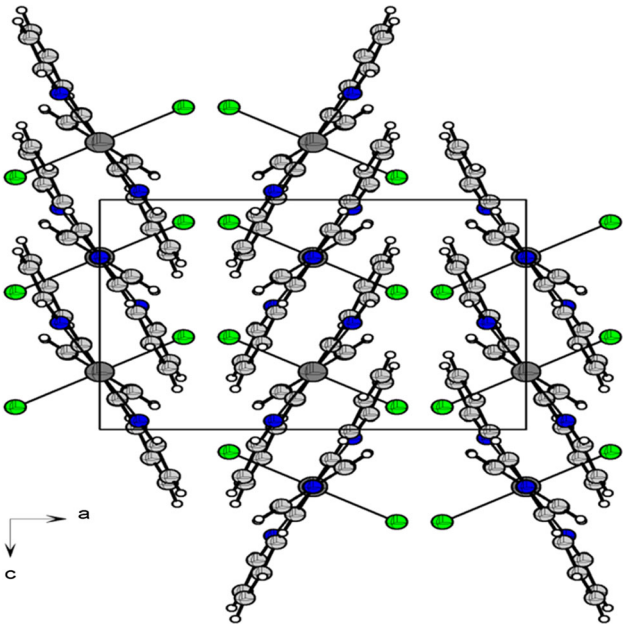

Fig. 4 Crystal structure of [$SnCl_2$(pytpy)] along the *b axis*

Experimental

All chemicals were reagent grade and were used as received. Elemental analyses were performed on a Perkin-Elmer 2400 II elemental analyzer. A Bante510 benchtop conductivity meter was used to test the conductance of prepared complexes **1–3** in water, acetone, and $CHCl_3$ solutions. IR spectra in the 4000–400 cm^{-1} were recorded on KBr pellet using ABB Bomem Model FTLA200-100 spectrophotometer. UV–Vis spectra of solutions recorded in quartz cuvettes using Analytic Jena SPECORD 210. NMR data were recorded using Bruker Biospin GmbH 500 MHz and Bruker FT-NMR300 (300 MHz) spectrometers. All the chemical shifts and coupling constants are reported in ppm and Hz, respectively. The ^{1}H, ^{13}C, and ^{119}Sn NMR spectra are reported relative to TMS (^{1}H, ^{13}C) and $SnMe_4$ (^{119}Sn). Calf thymus-DNA, 2-acetylpyridine, and 4-pyridylcarbaldehyde were purchased from Sigma-Aldrich and all substituted benzaldehydes, dimethyltin(IV) dichloride, and Tris-Base buffer were purchased from Merck.

*Preparation of ligands **L1–L6***

The one-pot preparation method of Kröhnke type 4′-aryl-2,2′:6′,2″-terpyridine ligands was performed to obtain ligands **L1–L5** according to the literature [23] with a slight modification. 2-Acetylpyridine (0.56 cm^3, 5.0 mmol) was added to a solution of 0.25 cm^3 benzaldehyde (2.5 mmol) in 18 cm^3 ethanol. After addition of the mixture of 0.280 g KOH (5.0 mmol) and 0.5 cm^3 NH_3 (25 %, 6.5 mmol), the solution was stirred overnight at room temperature, during which time as orange suspension was appeared. The solid was collected by filtration and washed with EtOH (3 × 6 cm^3). Then, the crude solid product was recrystallized by cooling the hot supersaturated ethanolic solution. The preparation method of diketone ligand (**L6**) was performed similar to the above procedure for the preparation of substituted phenyl terpyridines without the addition of ammonia. The prepared ligand was characterized in good agreement with the literature [24].

{Chlorodimethyl(4′-phenyl-2,2′:6′,2″-terpyridine-κ^3-N,N′,N″)tin(IV)} trichlorodimethylstannate(IV)
(**1**, $C_{25}H_{27}Cl_4N_3Sn_2$)

To a solution of 55 mg dimethyltin dichloride (0.25 mmol) in 5 cm^3 dichloromethane was added a solution of 77 mg Phtpy (**L1**, 0.25 mmol) in 5 cm^3 dichloromethane. The mixture was then stirred overnight at room temperature. In the case of soluble product, the solvent was evaporated to concentrate. Then, the solid was formed by the addition of diethyl ether. It was washed two times more with diethyl ether. Yield: 60 %; m.p.: 173–175 °C; IR (KBr): $\bar{\nu}$ = 3454 (w), 1610 (m), 1545 (m), 1478 (m), 1413 (m), 1253 (m), 1110 (m), 1021 (m), 890 (w), 797 (s), 765 (s), 689 (m) cm^{-1}; ^{1}H NMR ($CDCl_3$): δ = 8.88 (d, 2H, ^{3}J (HH) = 4.3 Hz, $H_{6,\ 6''}$), 8.78 (s, 2H, $H_{3',\ 5'}$), 8.73 (d, 2H, ^{3}J (HH) = 8.0 Hz, $H_{3,\ 3''}$), 7.99 (dt, 2H, ^{3}J (HH) = 11.0 Hz, ^{3}J (HH) = 4.5 Hz, $H_{4,\ 4''}$), 7.96 (d, 2H, ^{3}J (HH) = 7.2 Hz, $H_{Ph2,6}$), 7.55 (dd, 2H, ^{3}J = 7.2 Hz, ^{3}J (HH) = 5.9 Hz, $H_{5,\ 5''}$), 7.49 (dd, 1H, ^{3}J (HH) = 5.3 Hz, H_{Ph4}), 7.46 (dd, 2H, ^{3}J (HH) = 6.8 Hz, ^{3}J (HH) = 5.3 Hz, $H_{Ph3,5}$), 1.23 (s, 6H, ^{2}J ($^{119/117}$Sn–H) = 90.6 Hz, Me–Sn) ppm; ^{13}C NMR ($CDCl_3$): δ = 155.0 ($C_{2,\ 2''}$), 151.2 ($C_{2',\ 6'}$), 149.0 ($C_{6,\ 6''}$), 147.0 ($C_{4'}$), 138.0 (C_{Ph1}), 137.7 ($C_{4,\ 4''}$), 129.4 ($C_{Ph3,5}$), 129.1 (C_{Ph4}), 127.5 ($C_{Ph2,6}$), 124.4 ($C_{5,\ 5''}$), 121.9 ($C_{3,\ 3''}$), 119.5 ($C_{3',\ 5'}$), 16.8 (Me–Sn) ppm; ^{119}Sn NMR ($CDCl_3$): δ = −122 ppm.

{Chlorodimethyl[4′-(4-methylphenyl)-2,2′:6′,2″-terpyridine-κ^3-N,N′,N″]tin(IV)} chloride dihydrate
(**2**, $C_{24}H_{23}Cl_2N_3Sn{\cdot}2H_2O$)

Yield: 67 %; m.p.: 172–174 °C; IR (KBr): $\bar{\nu}$ = 3414 (br), 3037 (m), 2972 (m), 2920 (m), 2861 (m), 1603 (s), 1545 (m), 1476 (m), 1421 (m), 1396 (m), 1252 (w), 1112 (w), 1017 (w), 795 (s) cm^{-1}; ^{1}H NMR ($CDCl_3$): δ = 9.05 (d, 2H, ^{3}J (HH) = 4.4 Hz, $H_{6,\ 6''}$), 8.79 (d, 2H, ^{3}J (HH) = 9.9 Hz, $H_{3,\ 3''}$), 8.77 (s, 2H, $H_{3',\ 5'}$), 8.14 (t, 2H, ^{3}J (HH) = 7.7 Hz, $H_{4,\ 4''}$), 7.90 (d, 2H, ^{3}J (HH) = 8.1 Hz, $H_{Ph2,6}$), 7.59 (m, 2H, $H_{5,\ 5''}$), 7.36 (d, 2H, ^{3}J (HH) = 8.0 Hz, $H_{Ph3,5}$), 2.43 (s, 3H, Me-Ph), 1.20 (s, 6H, ^{2}J ($^{119/117}$Sn-H) = 93.2 Hz, Me-Sn) ppm; ^{13}C NMR ($CDCl_3$): δ = 152.9 ($C_{2,\ 2''}$), 152.3 ($C_{2',\ 6'}$), 148.6 ($C_{6,\ 6''}$), 140.7 (C_{Ph1}), 139.4 ($C_{4,\ 4''}$), 133.8 (C_{Ph4}), 130.1 ($C_{Ph3,5}$), 127.5 ($C_{Ph2,6}$), 125.6 ($C_{5,\ 5''}$), 123.1 ($C_{3,\ 3''}$), 120.2 ($C_{3',\ 5'}$), 21.4 (Me-Ph), 18.8 (Me-Sn) ppm; ^{119}Sn NMR ($CDCl_3$): δ = −64, −116 ppm.

{Chlorodimethyl[4′-(4-methoxyphenyl)-2,2′:6′,2″-terpyridine-κ^3-N,N′,N″]tin(IV)} trichlorodimethylstannate(IV)
(**3**, $C_{26}H_{29}Cl_4N_3OSn_2$)

Yield: 70 %; m.p.: 185–187 °C; IR (KBr): $\bar{\nu}$ = 3426 (br), 3062 (w), 3014 (w), 2922 (m), 2839 (w), 1600 (s), 1530 (m), 1478 (m), 1408 (m), 1249 (s), 1183 (s), 1016 (s), 794 (s) cm^{-1}; ^{1}H NMR ($CDCl_3$): δ = 9.35 (d, 2H, ^{3}J (HH) = 4.0 Hz, $H_{6,\ 6''}$), 9.07 (d, 2H, ^{3}J (HH) = 7.8 Hz, $H_{3,3''}$), 8.85 (s, 2H, $H_{3',\ 5'}$), 8.49 (t, 2H, ^{3}J (HH) = 7.5 Hz, $H_{4,\ 4''}$), 8.11 (d, 2H, ^{3}J (HH) = 8.5 Hz, $H_{Ph2,6}$), 7.87 (t, 2H, ^{3}J (HH) = 5.9 Hz, $H_{5,\ 5''}$), 7.01 (d, 2H, ^{3}J (HH) = 8.6 Hz, $H_{Ph3,5}$); 3.71 (s, 3H, Me-O), 1.21 (s, 12H, ^{2}J ($^{119/117}$Sn–H) = 92.5 Hz, Me–Sn) ppm; ^{13}C NMR ($CDCl_3$): δ = 162.2 (C_{Ph4}), 154.7 ($C_{2,\ 2''}$), 150.1 ($C_{2',\ 6'}$), 148.9 ($C_{4'}$), 147.9 ($C_{6,\ 6''}$), 141.7 ($C_{4,\ 4''}$), 129.8 ($C_{Ph2,6}$), 127.1 ($C_{5,\ 5''}$), 124.5 ($C_{3,\ 3''}$), 120.9 ($C_{3',\ 5'}$), 115.1 ($C_{Ph3,5}$), 55.5 (Me-O), 18.4 (^{1}J (^{119}Sn-C) = 787 Hz, ^{1}J (^{117}Sn-C) = 751 Hz, Me-Sn) ppm; ^{119}Sn NMR ($CDCl_3$): δ = −69, −121 ppm.

{Chlorodimethyl[4′-(4-chlorophenyl)-2,2′:6′,2″-terpyridine-κ^3-N,N′,N″]tin(IV)} trichlorodimethylstannate(IV) monohydrate (**4**, $C_{25}H_{26}Cl_5N_3Sn_2{\bullet}H_2O$)
Yield: 40 %; m.p.: 184–186 °C; IR (KBr): $\bar{\nu}$ = 3440 (br), 3065 (m), 3014 (w), 2917 (w), 1606 (s), 1543 (m), 1484 (s), 1427(m), 1397 (m), 1306 (w), 1251 (m), 1168 (w), 1088 (m), 1016 (s), 896 (w), 791 (s) cm^{-1}; ^1H NMR ($CDCl_3$): δ = 9.21 (d, 2H, ^3J (HH) = 4.8 Hz, $H_{6,\ 6''}$), 8.97 (d, 2H, ^3J (HH) = 8.0 Hz, $H_{3,3''}$), 8.81 (s, 2H, $H_{3',\ 5'}$), 8.34 (t, 2H, ^3J (HH) = 7.8 Hz, $H_{4,\ 4''}$), 8.01 (d, 2H, ^3J (HH) = 8.5 Hz, $H_{Ph2,6}$), 7.75 (t, 2H, ^3J (HH) = 6.3 Hz, $H_{5,\ 5''}$), 7.44 (d, 2H, ^3J (HH) = 8.6 Hz, $H_{Ph3,5}$), 1.23 (s, 12H, ^2J (^{119}Sn–H) = 89.5 Hz, ^2J (^{117}Sn–H) = 86.2 Hz, Me–Sn) ppm; ^{13}C NMR (acetone-d_6): δ = 155.7 ($C_{2,\ 2''}$), 154.6 ($C_{2',\ 6'}$), 150.9 ($C_{6,\ 6''}$), 149.9 ($C_{4'}$), 139.1 (C_{Ph1}), 137.3 ($C_{4,\ 4''}$), 136.2 (C_{Ph4}), 130.3 ($C_{Ph3,5}$), 129.8 ($C_{Ph2,6}$), 126.0 ($C_{5,\ 5''}$), 122.7 ($C_{3,\ 3''}$), 120.0 ($C_{3',\ 5'}$), 14.5 (Me–Sn) ppm; ^{119}Sn NMR (acetone-d_6): δ = -150, -632 ppm.

Dichloro[4′-(pyridine-4-yl)-2,2′:6′,2″-terpyridine-κ^3-N,N′,N″]tin(II) monohydrate (**5**, $C_{20}H_{14}N_4Cl_2Sn{\bullet}H_2O$)
Tin(II) chloride (29 mg, 0.15 mmol) was dissolved in THF and mixed with solution of 47 mg **L5** (0.15 mmol) in CH_2Cl_2. Immediately, an orange solid was appeared that stirred for 24 h and then discarded by centrifuge and washed with CH_2Cl_2. Yield: 78 %; m.p.: 266–268 °C; IR (KBr): $\bar{\nu}$ = 3409 (br), 2922 (w), 1747 (w), 1601 (m), 1536 (w), 1485 (w), 1407 (m), 1304 (w), 1251 (w), 1158 (w), 1091 (w), 1016 (m), 896 (w), 796 (s), 749 (m), 665 (s) cm^{-1}; ^1H NMR (DMSO-d_6): δ = 8.86 (s, 2H, $H_{3',\ 5'}$), 8.85-8.77 (m, 6H, $H_{3,\ 3''}$, $H_{6,\ 6''}$ and $H_{Py2,6}$), 8.14 (t, 2H, ^3J (HH) = 7.6 Hz, $H_{4,\ 4''}$), 8.01 (d, 2H, ^3J (HH) = 4.6, $H_{Py3,5}$), 7.64 (t, 2H, ^3J (HH) = 5.8 Hz, $H_{5,\ 5''}$) ppm; ^{13}C NMR (DMSO-d_6): δ = 155.4 ($C_{2,\ 2''}$), 150.6 ($C_{6,\ 6''}$), 149.0 ($C_{Py2,6}$), 147.5 ($C_{4'}$), 144.7 (C_{Py4}), 138.1 ($C_{4,\ 4''}$), 125.2 ($C_{5,\ 5''}$), 121.7 ($C_{3,\ 3''}$), 121.5 ($C_{Py3,5}$), 118.6 ($C_{3',\ 5'}$) ppm; ^{119}Sn NMR (DMSO-d_6): δ = −630 ppm.

{Chlorodimethyl[3-phenyl-1,5-bis(pyridine-2-yl)pentane-1,5-dione-κ^2-N,O]} chloride [3-phenyl-1,5-bis(pyridine-2-yl)pentane-1,5-dione] dichloromethane disolvate
(**6**, $C_{44}H_{42}Cl_2N_4O_4Sn{\bullet}CH_2Cl_2$)
Yield: 30 %; m.p.: 125–127 °C; IR (KBr): $\bar{\nu}$ = 3429 (br), 3057 (w), 2919 (w), 1692 (s), 1586 (m), 1492 (w), 1410 (m), 1357 (m), 1288 (m), 1223 (w), 1154 (w), 996 (s), 781 (s), 759 (s), 701 (s) cm^{-1}; ^1H NMR (acetone-d_6): δ = 8.68 (d, 2H, ^3J (HH) = 4.7 Hz, $H_{6,\ 6''}$), 7.94 (dt, 2H, ^3J (HH) = 7.8 Hz, ^4J (HH) = 1.6 Hz, $H_{4,4'}$), 7.91 (t, 2H, ^3J (HH) = 7.8 Hz, $H_{3,\ 3'}$), 7.59 (m, 2H, $H_{5,\ 5'}$), 7.38 (d, 2H, ^3J (HH) = 7.6 Hz, $H_{Ph2,6}$), 7.23 (t, 2H, ^3J (HH) = 7.3 Hz, $H_{Ph3,5}$), 7.11 (t, 1H, ^3J (HH) = 7.1 Hz, H_{Ph4}), 4.12 (qui, 1H, ^3J (HH) = 7.1 Hz, CH), 3.83 (dd, 2H, ^2J (HH) = 17.3 Hz, ^3J (HH) = 7.7 Hz, CH_2), 3.56 (dd, 2H, ^2J (HH) = 16.9 Hz, ^3J (HH) = 6.3 Hz, CH_2), 1.21 (s, 9H, ^2J ($^{119/117}$Sn–H) = 85.4 Hz, Me–Sn) ppm; ^{13}C NMR (acetone-d_6): δ = 200.5 (C=O), 154.9 (C_2), 154.2 ($C_{2'}$), 149.8 ($C_{6'}$), 148.8 (C_6), 145.8 (Ph_1), 138.0 ($C_{4'}$), 137.0 (C_4), 129.3 (Ph_4), 129.0 ($Ph_{3,5}$), 128.5 (C_3), 128.2 ($Ph_{2,6}$), 127.4 (C_5), 126.9 ($C_{5'}$), 121.6 ($C_{3'}$), 41.9 (CH_2), 37.2 (CH), 12.7 (Me–Sn, ^1J ($^{119/117}$Sn–C) = 845 Hz) ppm; distinguished ^{13}C NMR data for free **L6** (rather than common peaks): δ = 206.5 (C=O), 128.6, 128.3, 122.1, 44.5 (CH_2) ppm; ^{119}Sn NMR (acetone-d_6): δ = 10 ppm.

UV–Vis absorption spectra of DNA solutions

The stock solution of ct-DNA was prepared in Tris-Base buffer, adjusted at neutral pH and stored overnight at 4 °C. Solutions of ct-DNA and complex were scanned using quartz cuvettes. The concentration of the nucleotide was determined by UV–Vis absorption spectroscopy using the molar absorption coefficient (ε = 6600 M^{-1} cm^{-1}) at 260 nm. Absorbance measurements were performed by keeping the constant concentration of complex **5** (30 μM) while varying the ct-DNA concentration. The samples were incubated at room temperature for 7 min before each spectral determination. Also, in other sample, time dependent absorbance determination was performed by

Table 2 Experimental details, crystal data and refinement parameters for complex **5**

Chemical formula	$C_{20}H_{14}Cl_2N_4Sn$
Formula weight/g mol^{-1}	499.96
Crystal system, space group	Orthorhombic, *Pbcn*
Temperature/K	295
a/Å	11.485 (2)
b/Å	18.360 (4)
c/Å	9.1006 (18)
V/Å^3	1919.0 (7)
Z	4
F(000)	984
Dx/Mg/m^{-3}	1.731
Radiation type	Mo *Kα*, λ = 0.71073/Å
μ/mm^{-1}	1.62
Crystal size/mm	0.22 × 0.14 × 0.13
No. of measured, independent and observed [$I > 2\sigma(I)$] reflections	6372, 1880, 1657
R_{int}	0.040
(sin $\theta/\lambda)_{max}$/Å^{-1}	0.617
$R[F^2 > 2\sigma(F^2)]$, wR(F^2), *S*	0.034, 0.082, 1.07
No. of reflections	1880
No. of parameters	125
H-atom treatment	H atoms treated by a mixture of independent and constrained refinement
$\Delta\rho_{max}$, $\Delta\rho_{min}$/e Å^{-3}	0.38, −0.46

keeping constant concentration of both metal complex and ct-DNA (1:1), in given periods (Fig. 2).

X-ray crystal structure determination

Red single crystals of complex **5** were grown from slow diffusion of THF solution of tin(II) chloride into hot methanol solution of ligand **L5** (reactant diffusion method). Crystallographic data were collected on an MAR345 dtb diffractometer equipped with image plate detector using Mo Kα X-ray radiation. The structures were solved by direct methods using SHELXS-97 and refined using full-matrix least-squares method on F^2, SHELXL-97 [45]. All non-hydrogen atoms were refined anisotropically. Hydrogen atoms were added at ideal positions and refined using a riding model. A summary of crystal data, experimental details, and refinement results is given in Table 2. CCDC 995748 contains the supplementary crystallographic data for this paper. These data can be obtained free of charge via http://www.ccdc.cam.ac.uk/conts/retrieving.html, or from the Cambridge Crystallographic Data Centre, 12 Union Road, Cambridge CB2 1EZ, UK; fax: (+44) 1223-336-033; or e-mail: deposit@ccdc.cam.ac.uk. Other supplementary data related to this article is also available.

Acknowledgments We thank the Science Research Council of K. N. Toosi University of Technology for financial support.

References

1. Newkome GR, Guther R, Moorefield CN, Cardullo F, Echegoyen L, Perez-Cordero E, Luftmann H (1995) Angew Chem Int Ed 34:2023
2. Newkome GR, He E (1997) J Mater Chem 7:1237
3. Newkome GR, Yoo KS, Moorefield CN (2002) Chem Commun 2164
4. Blasini DR, Flores-Torres S, Smilgies DM, Abruna HD (2006) Langmuir 22:2082
5. Maskus M, Abruna HD (1996) Langmuir 12:4455
6. Schubert US, Andres PR, Hofmeier H (2001) Polym Mater Sci Eng 85:510
7. Schubert US, Eschbaumer C (2002) Angew Chem Int Ed 41:2892
8. Andres PR, Schubert US (2004) Adv Mater 16:1043
9. Shunmugam R, Gabriel GJ, Aamer KA, Tew GN (2010) Macromol Rapid Commun 31:784
10. Lohmeijer BGG, Schubert US (2005) J Polym Sci Part A Polym Chem 43:6331
11. Fustin CA, Guillet P, Schubert US, Gohy JF (2007) Adv Mater 19:1665
12. Whittle GR, Hager MD, Schubert US, Manners I (2011) Nat Mater 10:176
13. Chiper M, Hoogenboom R, Schubert US (2009) Macromol Rapid Commun 30:565
14. Heller M, Schubert US (2003) Eur J Org Chem 947
15. Davies AG, Gielen M, Pannell KH, Tiekink ERT (eds) (2008) Tin chemistry: fundamentals, frontiers, and applications. Wiley, Chichester
16. Hadjikakou SK, Hadjiliadis N (2009) Coord Chem Rev 253:235
17. Gielen M (2002) Appl Organomet Chem 16:481
18. Gielen M, Tieknik ERT (2005) Metallotherapeutic drugs and metal-based diagnostic agents: the use of metals in medicine. Wiley, Chichester
19. Dabrowiak JC (2009) Metals in medicine. Wiley, Chichester
20. Constable EC, Lewis J, Liptrot MC, Raithby PR (1984) J Chem Soc Dalton Trans 2177
21. Shi PF, Jiang Q, Duan HC, Wang DQ (2014) Chin Chem Lett 25:586
22. Momeni BZ, Jebraeil SM, Patrick BO, Abd-El-Aziz AS (2013) Polyhedron 55:184
23. Wang J, Hanan GS (2005) Synlett 2005(8):1251
24. Constable EC, Lewis J, Liptrot MC, Raithby PR (1990) Inorg Chim Acta 178:47
25. Lockhart TP, Manders WF (1987) J Am Chem Soc 109:7015
26. Tobias RS (1970) Inorg Chem 9:1296
27. Manders WF, Lockhart TP (1985) J Organomet Chem 297:143
28. Lockhart TP, Manders WF (1986) Inorg Chem 25:892
29. Lockhart TP, Manders WF, Zuckerman JJ (1985) J Am Chem Soc 107:4546
30. Barbieri G, Taddei F (1972) J Chem Soc Perkin Trans 2:1327
31. Friebolin H (2005) Basic one- and two- dimensional NMR spectroscopy. Wiley, Weinheim
32. Otera J, Hinoishi T, Okawara R (1980) J Organomet Chem 202:C93
33. Colton R, Dakternieks D (1988) Inorg Chim Acta 148:31
34. Casella G, Ferrante F, Saielli G (2008) Inorg Chem 47:4796
35. Chen GJ, Wang ZG, Kou YY, Tian JL, Yan SP (2013) J Inorg Biochem 122:49
36. Shahabadi N, Nemati L (2012) DNA Cell Biol 31:883
37. Siddiqi ZA, Sharma PK, Shahid M, Khalid M (2013) J Photochem Photobiol B: Biol 125:171
38. Tabassum S, Ahmad Khan R, Arjmand F, Sen S, Kayal J, Juvekar AS, Zingde SM (2011) J Organomet Chem 696:1600
39. Arvin M, Dehghan G, Hosseinpourfeizi MA, Moosavi-Movahedi AA (2013) Spectrosc Lett 46:250
40. Karami K, Lighvan ZM, Barzani SA, Faal AY, Poshteh-Shirani M, Khayamian T, Eignerc V, Dusekc M (2015) New J Chem 39:8708
41. Addison AW, Rao TN, Reedijk J, van Rijn J, Vershoor GC (1984) J Chem Soc Dalton Trans 1349
42. Long XJ, Dai JW, Wu JZ (2012) J Coord Chem 65:316
43. Zubieta JA, Zuckerman JJ (1978) Prog Inorg Chem 24:251
44. Archer SJ, Koch KR, Nassimbeni LR (1986) J Cryst Spect Res 16:449
45. Sheldrick GM (1997) SHELXS97 and SHELXL97. University of Göttingen, Germany